Image Threshold Segmentation with Jensen-Shannon Divergence and Its Application

Fangyan Nie, *Member*, *IAENG*, and Jianqi Li

Abstract—**Thresholding based on information divergence is an important technique for image segmentation. It has been applied successfully in many fields because of its excellent performance. Due to its nonsymmetrical characteristic, the traditional information divergence has some shortcomings in measuring the similarity between different probability distributions. Compared with the traditional information divergence, the Jensen-Shannon divergence is more accurate in measuring the similarity of probability distribution. Based on this, a Jensen-Shannon divergence thresholding method for image segmentation is proposed. In the proposed method, the Jensen-Shannon divergence of the segmented image is constructed according to the gray level distribution information of the image pixels, and the optimal segmentation threshold is calculated according to the principle of minimum divergence. Finally, the proposed method is applied to the segmentation of non-destructive testing images and medical images, and compared with the traditional divergence threshold segmentation method and some classical methods. Experimental results show that the proposed method achieves good segmentation results, and the computation time is less than 1 seconds for images with size less than 576×768. Therefore, the proposed method has a good application prospect and promotion value in scenarios with high real-time performance requirements.**

Index Terms—**image segmentation, thresholding, Jensen-Shannon divergence, non-destructive testing image, medical image**

I. Introduction

As the basic and key technology of image processing, image segmentation plays an important role in modern industrial production, such as workpiece surface defect detection based on nondestructive testing [1], medical auxiliary diagnosis [2-3], agricultural product quality monitoring and evaluation [4], forest vegetation monitoring and protection [5], etc. Due to the complexity and diversity of the real production environment, image segmentation is one of the most active technical branches in the field of image processing. In order to adapt to different processing tasks, the segmentation technologies based on various discipline background knowledge and principles have been developed continuously [6-8].

In many scenarios, such as product defect detection in production process flow operation [9-10] and real-time alarm of safety monitoring [11], the whole task needs to respond in time. To achieve this goal, the time-consuming performance of image processing must be regarded as an important consideration index. The threshold segmentation method based on image histogram information is widely used in scenes with high real-time requirements because of its low computational complexity, easy implementation and good segmentation accuracy.

Since the image processing technology is applied to the production scenario, the threshold segmentation method based on histogram information is also booming. Some mature threshold segmentation schemes with good performance have been widely used in the field of modern industrial production, such as Otsu method [12], minimum error method [13], and method based on information entropy [14-15] and so on. Among these methods, the cross entropy method based on information theory has been widely studied and applied in practice [16-18]. Cross entropy, also known as relative entropy, information divergence or Kullback-Leibler divergence (KL divergence), was first introduced into the field of image segmentation by Li and Lee [16]. Because of its good performance, the technology has been vigorously promoted and developed in nondestructive testing, medical diagnosis, target detection and other industries. KL divergence has the properties of nonnegativity and asymmetry. In essence, KL divergence is a similarity measure criterion used to measure two probability distributions. When measuring two probability distributions, if the points on the two probability distributions are far away, the divergence value calculated by KL divergence is meaningless. Based on the study of KL divergence by different scholars, a symmetric version of divergence measurement criterion is proposed. In many literatures, this divergence is called Jensen-Shannon divergence or JS divergence [19]. JS divergence overcomes the shortcomings of KL divergence in measuring the similarity of probability distribution. Compared with KL divergence, JS divergence is more accurate in judging the similarity of probability distribution. Because JS divergence has better performance than KL divergence, it has been successfully applied in many frontier research fields, such as generative adversarial network in deep learning.

Based on JS divergence, this paper proposes a thresholding method for image segmentation, and compares the proposed method with the traditional KL divergence

Manuscript received October 5, 2021; revised December 24, 2021. This work was supported in part by the Research Foundation of Department of Education of Hunan Province, China (Grant No.18A368) and the Natural Science Foundation of Hunan Province, China (Grant No.2021JJ50022, 2021JJ30477).

Fangyan Nie is a Professor of College of Computer and Electrical Engineering, Hunan University of Arts and Sciences, Hunan, 415000 China (corresponding author phone: +86-736-7187895; e-mail: niefyan@huas.edu.cn)

Jianqi Li is a Professor of College of Computer and Electrical Engineering, Hunan University of Arts and Sciences, Hunan, 415000 China (e-mail: li_jianqi@126.com).

thresholding method and some methods widely and successfully used in image segmentation, such as Otsu method [12], minimum error method [13] and maximum entropy method [14], in the application of nondestructive testing image and medical image segmentation.

II. Jensen-Shannon divergence

Let $\Gamma=\{P=(p_1,p_2,\ldots,p_n)\}$ be a complete set of finite discrete probability distributions, where $p_i>0$, $\Sigma p_i=1$, $n\geq 2$. Let $P,Q\in\Gamma$, JS divergence as a measurement criterion to measure the similarity between different probability distributions, and its definition is shown in equation (1).

$$D(P\,|\,Q)=\sum_{i=1}^{n} p_i \ln\left(\frac{2p_i}{p_i+q_i}\right) \qquad (1)$$

III. Principles of Image Segmentation

Let $\boldsymbol{I}$ be a digital image to be segmented, and its size is $m\times n$. In addition, let $\boldsymbol{G}$ be the gray level set of the image, $\boldsymbol{G}=\{g_0,g_1,\ldots,g_L\}$, L=255, g_0=0, g_1=1, …, g_L=255, for 8-bit digital images (unless otherwise specified, the images mentioned below are 8-bit digital images). Let the number of pixels appearing in the gray level i in the image $\boldsymbol{I}$ be h_i, that is, the frequency of the gray level i in the image $\boldsymbol{I}$. Counting h_i, you can get the frequency set of all gray levels of image $\boldsymbol{I}$, here we use $\boldsymbol{H}$ to denote, that is, $\boldsymbol{H}=\{h_0,h_1,\ldots,h_L\}$.

A. Thresholding criterion function

In the process of image thresholding, let t be the threshold value obtained, then the thresholding process can be expressed by equation (2).

$$f(t)=\begin{cases} g_0, & \mathrm{g}_t\leq t \\ g_L, & g_t>t \end{cases} \qquad (2)$$

Here, $f(t)$ represents the pixel gray value of the segmented image, g_t represents the pixel gray value of the image to be segmented.

In order to construct the thresholding criterion function, the following conventions are made when the proposed method is used to image segmentation. Let t as an optimal threshold for image thresholding. The threshold t divides the image gray level into two categories, one is defined as $C0=\{g_0,g_1,\ldots,g_t\}$, and the other is defined as $C1=\{g_{t+1},g_{t+2},\ldots,g_L\}$. At the same time, normalizing the image frequency set $\boldsymbol{H}$, we can get $\boldsymbol{P}=\{p_0,p_1,\ldots,p_L\}$, $p_i=h_i/(m\times n)$. Here, $\boldsymbol{P}$ can be expressed as the frequency probability set of image $\boldsymbol{I}$.

Let $\Pi_0=\{p_0,p_1,\ldots,p_t\}$,$\Pi_1=\{p_{t+1},p_{t+2},\ldots,p_L\}$ denote the gray-level frequency probability set of $C0$ and $C1$, and use $\omega_0= p_0+p_1+\ldots+p_t$, $\omega_1= p_{t+1}+p_{t+2}+\ldots+p_L$ represents the total gray-level frequency probability of $C0$ and $C1$. At the same time, let m_0, m_1 respectively denote the average gray level values of pixels about $C0$ and $C1$, namely

$$m_0=\frac{1}{\omega_0}\sum_{i=0}^{t} p_i g_i \qquad (3)$$

$$m_1=\frac{1}{\omega_1}\sum_{i=t+1}^{L} p_i g_i \qquad (4)$$

On the basis of the above assumptions, define the JS divergence $D0$ and $D1$ of $C0$ and $C1$. The values of $D0$ and $D1$ can be calculated according to equation (1), namely

$$D0=\sum_{i=0}^{t} p_i\left(g_i\left(\ln\left(\frac{2g_i}{g_i+m_0}\right)\right)\right) \qquad (5)$$

$$D1=\sum_{i=t+1}^{L} p_i\left(g_i\left(\ln\left(\frac{2g_i}{g_i+m_1}\right)\right)\right) \qquad (6)$$

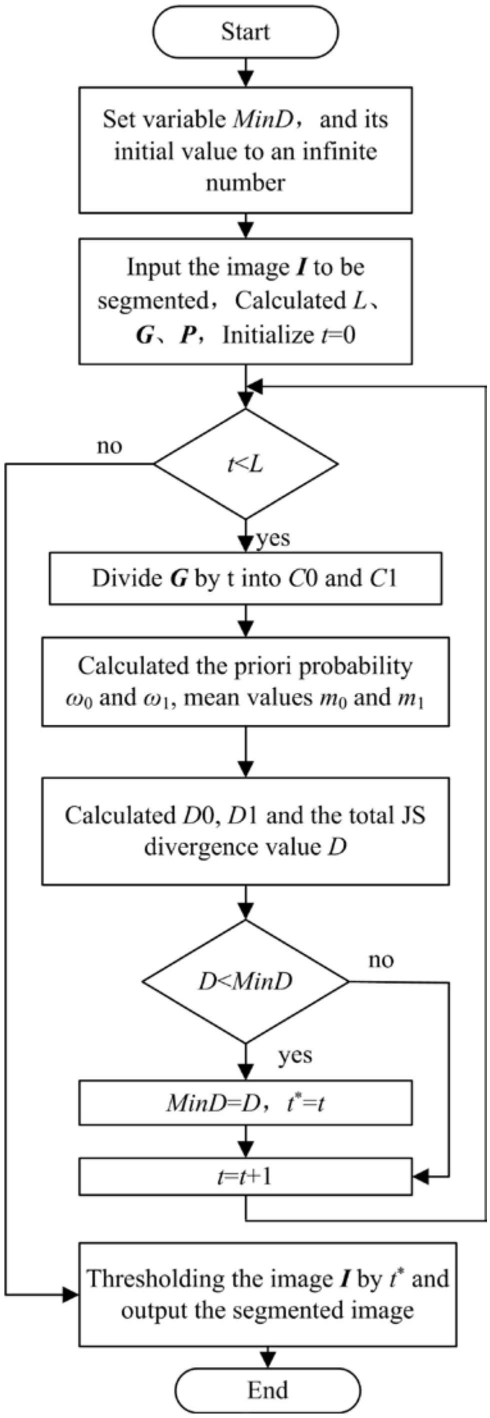

Fig.1 Algorithm flow chart of image thresholding

Then, the total JS divergence D of the image can be calculated by equation (7).

$$D=D0+D1 \qquad (7)$$

Suppose that when the image is thresholded, the optimal segmentation threshold is t^*. According to the principle of JS divergence, if the two probability distributions are more similar, the JS divergence value is smaller. Based on this, the image thresholding criterion function can be defined as

$$t^* = \arg\min_{t\in\mathbf{G}}(D) \tag{8}$$

B. Algorithm flowchart

When the method proposed in this paper is used for image threshold segmentation, the algorithm flow is shown in Figure 1.

IV. Analysis and Comparison of Experimental Results

In order to verify the effectiveness of the proposed method, in the research of this paper, the proposed method is compared with the traditional information divergence method, that is, the minimum cross entropy method [16]. At the same time, the Otsu method [12], the minimum error method [13], and the maximum entropy method [14], which achieve great success in many application scenarios, have also been compared and studied.

In this paper, the implementations of the all methods are based on the Windows 10 platform 64-bit system, the machine hardware configuration is Intel(R) Core(TM) i7-8550U CPU @1.80GHz 1.99 GHz processor, 16.0 GB RAM; programming implementation uses Python+ OpenCV environment, the software development tool platform is Visual Studio Code, and the software versions of this environment are Python 3.9.3, opencv-python 4.5.1.48, numpy 1.20.2, matplotlib 3.4.1, and Visual Studio Code 1.56.2.

A. Performance evaluation

Due to the complexity and diversity of images, there is no absolute "gold standard" for the performance evaluation of image segmentation algorithms. In this paper, we adopt the image pixel misclassification rate *MR*, which is the most intuitive and easiest to illustrate the "good or bad" performance of segmentation algorithm, as an objective evaluation standard. Image pixel misclassification rate *MR* is defined [20] as follows.

$$MR = \frac{\begin{array}{c}\text{Number of image pixels}\\ \text{that was misclassified}\end{array}}{\begin{array}{c}\text{The total number of pixels}\\ \text{in the image}\end{array}} \times 100\% \tag{9}$$

In equation (9), the number of misclassified image pixels refers to the number of pixels that should have been classified as background (target) pixels but were wrongly classified as target (background) pixels in the image segmentation process. Therefore, for equation (9), the smaller the value is, the better the performance of the segmentation algorithm will be. For the compared image segmentation algorithms, if this criterion is selected as the performance evaluation standard of the algorithm, it is necessary to have a more "perfect" reference segmentation image. These reference images are generally segmented images obtained by expert segmentation results or excellent algorithms with strong persuasiveness.

In modern industrial production, some processes require high real-time performance, for example, in intelligent manufacturing scenarios such as machine vision-based non-destructive testing. In these scenarios, the high real-time performance advantages of the image threshold segmentation method will be perfectly reflected in the task realization process. During the experiment, the method proposed in this paper was first applied to the segmentation of non-destructive testing images. In the selection of test images, considering the objective and fairness of the evaluation, some NDT images from reference [21] were selected in this subsection. Using these images to compare the performance of segmentation algorithms has been recognized by many researchers. These images not only have the original image to be segmented, but also have the result image manually segmented by the expert specialized for performance evaluation. Therefore, it is very convenient to compare the performance of each algorithm objectively based on *MR* criterion.

Here, we choose four NDT images to compare the algorithm performance. For convenience, the four images are named NDT-image1, NDT-Image2, NDT-image3 and NDT-Image4 respectively. The original images are shown in Figure 2. The sizes of these four images are 51×98, 51×88, 92×107 and 58×171 respectively, and their gray level histograms are shown in Figure 3. The groundtruths of four NDT images are shown in Figure 4.

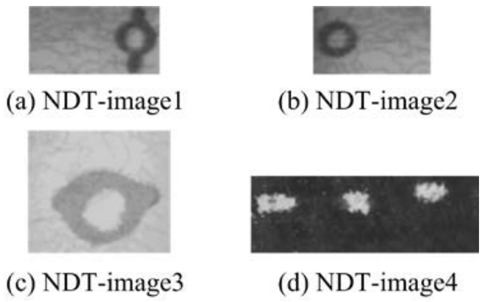

Fig.2 NDT images for testing

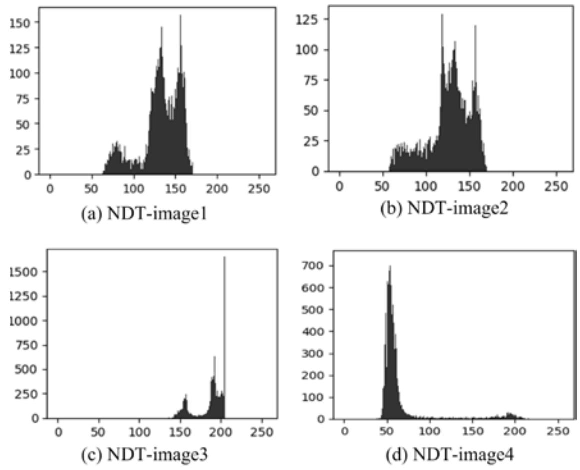

Fig.3 The gray-level histograms of NTD-images

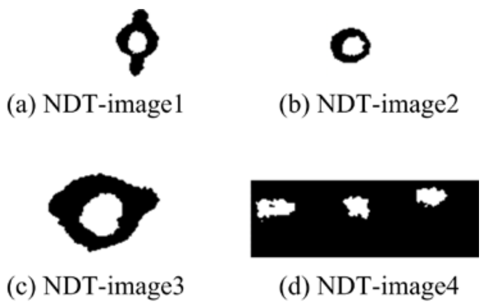

Fig.4 The groundtruths of NDT images for testing

As can be seen from Fig. 2, the proportion of target pixels in the four NDT images to be segmented is relatively low, and some pixels are fused with the background. It can also be seen from Fig. 3 that the gray level histogram distributions of these four images present irregular distribution patterns, including single-peak, double-peak and multi-peak distribution patterns. In general, when these images are segmented using thresholding methods, there is a certain degree of difficulty.

In the experiment, in addition to the Otsu method, minimum cross entropy method, minimum error method and maximum entropy method mentioned above, the method proposed by Xue et al. is also compared with the method proposed in this paper. According to the description of reference [22], the method proposed by Xue et al. has achieved good results in the segmentation of NDT images. For the sake of convenience, these methods are respectively referred to as Otsu method, MCE method, MET method, MaxE method, Xue method and the proposed method in the following sections. Fig. 5-8 lists the segmented results of NDT images obtained by these methods.

Fig. 5 shows the segmented results of NDT-image1. Compared with the groundtruth of NDT-image1 shown in Fig. 4, it can be seen from Fig. 5 that the results obtained by MCE method and the proposed method are better than those obtained by other methods. The results obtained by Otsu method and MaxE method are slightly inferior to those obtained by MCE method and the proposed method. The worst results were obtained by MET method and Xue method.

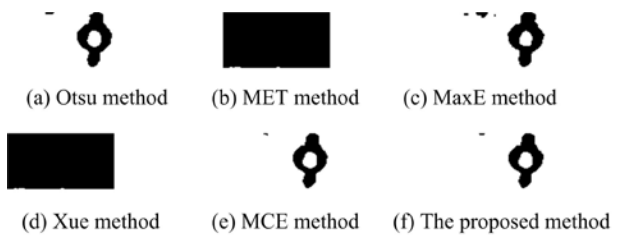

Fig.5 The segmented results of NDT-image1

Fig. 6 shows the segmented results of NDT-image2. It can be seen from Fig. 6 that there are shortcomings in all methods. Comparatively speaking, Xue method achieves a better result, but it is slightly over-segmented. The result of MET method is also good, but there are some noise pixels in the segmented result. The results obtained by the proposed method and MCE method are inferior to those obtained by Xue method and MET method, and there are more noise pixels in the results. The worst results were obtained by MaxE method.

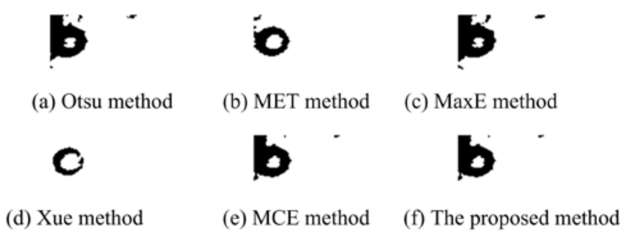

Fig.6 The segmented results of NDT-image2

Fig. 7 lists the segmented results of NDT-image3 for each method. As can be seen from Fig. 7, the results obtained by Otsu method, MCE method and the proposed method are roughly similar. Compared with Fig. 4, the results obtained by these three methods are basically the same as the groundtruth of NDT-image3. The results obtained by MET method and Xue method are relatively poor, and the real object in the image cannot be distinguished basically. For the MaxE method, there are many noise pixels in the results of this method.

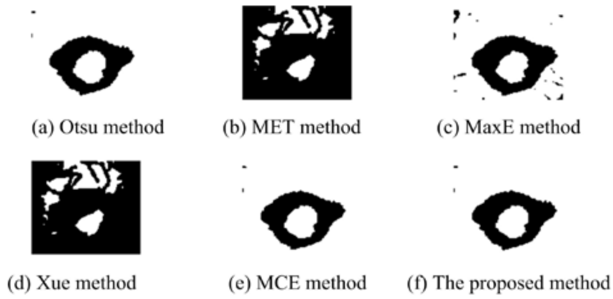

Fig.7 The segmented results of NDT-image3

Fig. 8 lists the segmented results of each method on NDT-image4. Compared with the groundtruth of NDT-image4 in Fig. 4, it can be seen from Fig. 8 that the results obtained by the proposed method, MCE method, and Otsu method are better than those obtained by the MET method, MaxE method, and Xue method.

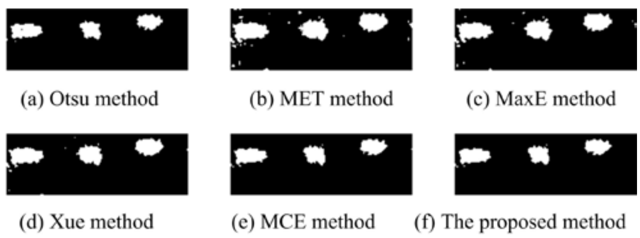

Fig.8 The segmented results of NDT-image4

Table I lists the optimal segmentation thresholds obtained by each method on four NDT images.

TABLE I
THE OPTIMAL THRESHOLDS FOR NDT IMAGES

Method	NDT-image1	NDT-image2	NDT-image3	NDT-image4
Otsu	113	112	175	115
MET	169	91	203	71
MaxE	117	114	183	76
Xue	169	78	203	83
MCE	110	108	174	101
Proposed	111	108	175	106

It can be seen from Table I, the optimal thresholds obtained by the proposed method are close to those obtained by the minimum cross entropy method (MCE method). The MCE method has achieved many successful applications in practical scenarios. The optimal thresholds obtained by the proposed method are similar to that of the MCE method, which proves the validity of the proposed method from another aspect. Compared with the gray level histograms shown in Fig. 3, the optimal thresholds obtained by the proposed method, MCE method, Otsu method and MaxE method are closer to the valley of the histogram distributions. When the thresholding method is applied to image segmentation, the threshold located near the trough region of the histogram distribution can achieve better segmentation effect. From the perspective of visual observation, this point is also relatively consistent with the segmented results in Fig. 5-8.

Table II lists the results of pixel misclassification rate *MR* values of each method on the segmentation of NDT images.

TABLE II
THE COMPARISON OF *MR* VALUES OF SEGMENTED RESULTS FOR NDT IMAGES

Method	NDT-image1	NDT-image2	NDT-image3	NDT-image4
Otsu	0.01961	0.12366	**0.00122**	**0.00756**
MET	0.85854	0.02830	0.59275	0.05051
MaxE	0.03842	0.13570	0.03545	0.03922
Xue	0.85854	**0.02028**	0.59275	0.03075
MCE	**0.01341**	0.10183	0.00406	0.01563
Proposed	0.01441	0.10183	**0.00122**	0.01240

As can be seen from Table II, the Otsu method obtains the minimum *MR* value on NDT-image3 and NDT-image4, the proposed method obtains the minimum *MR* value on NDT-image3, and the Xue method obtains the minimum *MR* value on NDT-image2. The MCE method obtains the minimum *MR* value on ndT-imag1. If the number of the first and second smallest *MR* values on each image is counted, the number is 3 for the proposed method, that is, the *MR* values obtained by the proposed method on NDT-image1, NDT-image3 and NDT-image4 are the smallest or the second smallest. Other methods only obtain the smallest or second smallest *MR* value on one or two images. From this point, the result obtained by the proposed method is slightly better than those obtained by other methods.

In industrial applications, the task processing based on machine vision requires real-time feedback in many scenarios. Therefore, the time performance of the processing system in these scenarios is also a factor that must be considered. Threshold segmentation methods generally consume less time, so in these scenarios, compared with other time-consuming algorithms, image threshold segmentation methods have been more widely used in practice. Here, in order to verify the time-consuming performance of each method compared in this paper, Table III lists the calculation time-consuming of each method for threshold segmentation of four NDT images.

TABLE III
THE COMPARISON OF TIME CONSUMING OF THRESHOLD SEGMENTATION FOR NDT IMAGES (SECOND)

Method	NDT-image1	NDT-image2	NDT-image3	NDT-image4
Otsu	0.0770	0.0650	0.1340	0.0584
MET	0.0289	0.0249	0.0456	0.0264
MaxE	0.0174	0.0169	0.0288	0.0160
Xue	0.0219	0.0189	0.0311	0.0200
MCE	0.0164	0.0147	0.0250	0.0170
Proposed	0.0170	0.0159	0.0249	0.0167

As can be seen from Table III, for the four tested NDT images, the time of segmentation of the six methods is all less than 0.1 seconds. In comparison, the proposed method, MCE method and MaxE method need less computing time. Therefore, in terms of time performance, the proposed method can meet the application scenarios with high real-time performance requirements.

B. Medical image segmentation experiment

In medical diagnosis, if image processing technology can be successfully applied in medical image processing, the complexity of medical image file processing by medical staff can be greatly reduced and the efficiency and accuracy of medical diagnosis can be improved [23]. Threshold segmentation method based on image cross entropy has also been successfully and widely used in medical practice [24]. Here, we apply the proposed method to medical image segmentation to further verify the performance and application prospects of the proposed method.

Fig. 9 shows a blood cell image and a medical human chromosome [2] image.

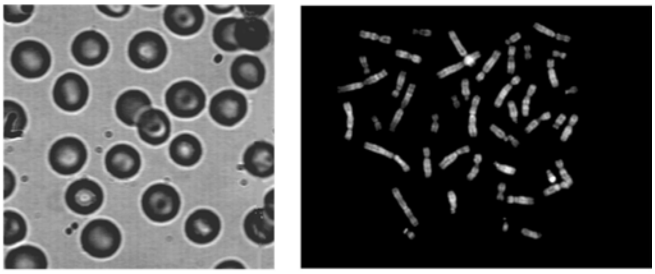

(a) Blood cell (b) Chromosome

Fig.9 Medical images

In clinical pathological examination, the classification and statistics of blood cells is an important and complicated work. In these scenarios, medical image analysis technology is often used for auxiliary statistical analysis. Chromosome karyotype analysis through chromosome structure visualization is a lengthy and repetitive but very important work in the clinical diagnosis of genetic defects. The work intensity of doctors can be greatly alleviated by using an effective and automatic machine vision based system for auxiliary analysis. Image segmentation is a basic work to realize the whole function of auxiliary diagnosis system in the above mentioned conventional medical clinical auxiliary diagnosis system. In these image segmentation tasks, considering the overall time response performance, the system mostly achieves the purpose of medical image segmentation through thresholding.

Fig. 10 shows the gray-level histograms of medical blood cell images and medical human chromosome images. As can be seen from Fig. 10, the pixel gray level distribution of the two images is very uneven and sparse. For the blood cell image, the gray level distribution presents an irregular bimodal distribution without obvious trough point. For the chromosomal image, the gray level distribution presents a very malformed single-peak distribution. A large number of image pixels are gathered at 0 gray level, while the number of pixels at other gray levels is very small.

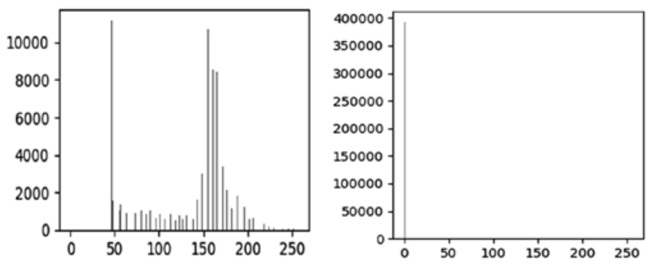

(a) Blood cell **(b) Chromosome**

Fig.10 The histograms of medical images

Table IV lists the optimal thresholds obtained by each method for the segmentation of two medical images and the time required for the completion of segmentation. Here, the size of the medical blood cell image is 265×272, and the size of a medical human chromosome image is 576×768.

It can be seen from Table IV, the optimal thresholds obtained by Otsu method, MCE method and the proposed method are similar on blood cell images. The optimal thresholds obtained by MaxE method, MCE method and the proposed method are similar on chromosome images. Compared with the histograms shown in Fig. 10, the threshold values obtained by these methods fall near the valley point of the histograms. Judging from the gray level histogram of the image, the segmentation results obtained by these methods should be good. In addition, it can also be seen from Table IV that the proposed method has a comparative advantage over other methods on computing time in the segmentation of two medical images. Even for the medical chromosome image with a size of 576×768, it does not take more than 1 second.

TABLE IV
THE COMPARISON OF OPTIMAL THRESHOLDS AND TIME CONSUMING (SECOND) FOR MEDICAL IMAGES SEGMENTATION

Method	Blood cell image		Chromosome image	
	Threshold	Computing time	Threshold	Computing time
Otsu	106	0.4971	60	1.8488
MET	46	0.2386	0	1.1616
MaxE	171	0.1449	16	0.8903
Xue	46	0.1889	0	1.0351
MCE	96	0.1628	13	0.9827
Proposed	101	0.1623	22	0.9882

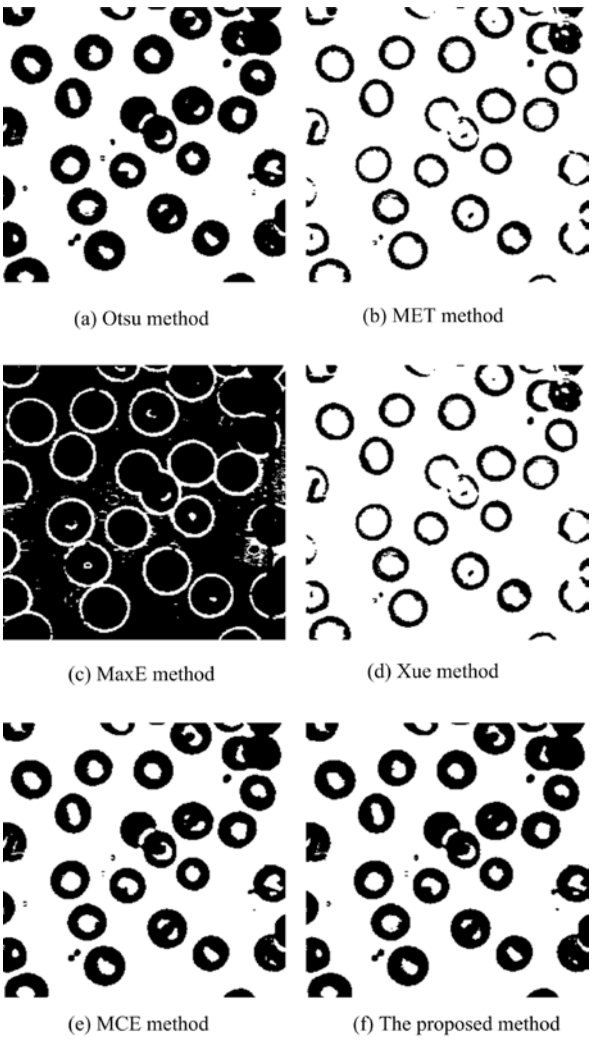

Fig.11 The segmented results of blood cell image

Fig. 11-12 show the segmented results of medical blood cell images and chromosome images by the six methods mentioned in this paper.

As can be seen from Fig. 11, the MET method and Xue method appear under-segmentation phenomenon for blood cell image segmentation, while the MaxE method appears over-segmentation phenomenon. Otsu method, MCE method and the proposed method have better results on blood cell segmentation.

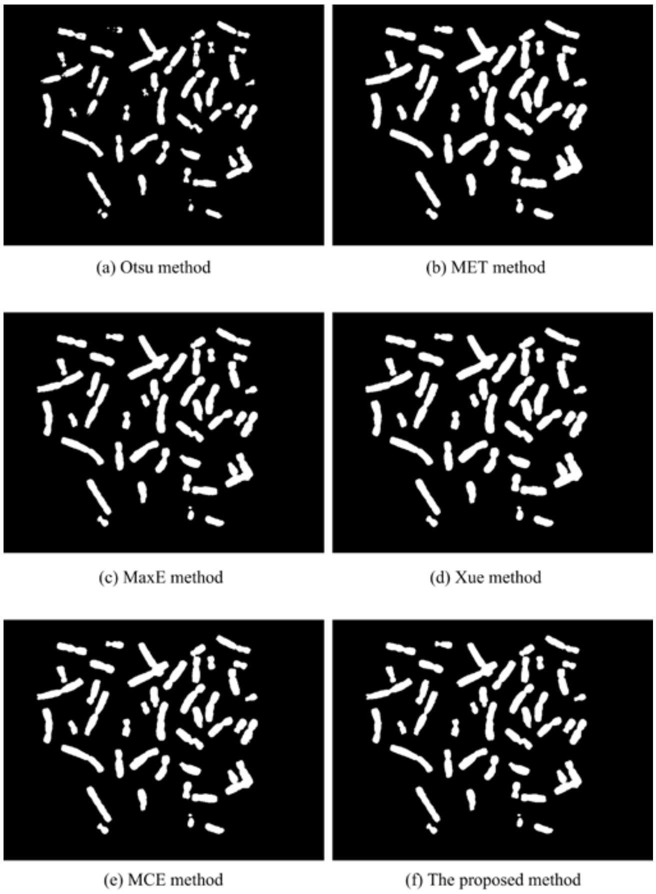

Fig.12 The segmented results of chromosome image

As can be seen from Fig. 12, the Otsu method shows over-segmentation phenomenon for chromosome image segmentation, and some chromosomes are broken and discontinuous after segmentation. The optimal thresholds obtained by MET method and Xue method were both 0 on chromosome image. By observing the segmented results, some chromosomes appeared adhesion. The segmented results obtained by MaxE method, MCE method and the proposed method are better.

V. CONCLUSION

Using information divergence (cross entropy) as a criterion function for image thresholding is a technique that is widely used and has achieved great success in the field of image segmentation. Traditional information divergence has some shortcomings in measuring the similarity of probability distribution because of its asymmetry. Based on this, this paper proposes a thresholding method for image segmentation based on Jensen Shannon divergence, which overcomes the deficiency of traditional information divergence. The proposed method is applied to the segmentation of industrial nondestructive testing images and some medical images. The effectiveness of the proposed method is verified by comparison with other methods.

Experiments on a large number of images show that the optimal threshold obtained by the proposed method is generally between the well-known maximum interclass variance method (Otsu method) and the minimum cross entropy method (MCE method), which can make up for the shortcomings of Otsu method and MCE method. In addition, for the method proposed in this paper, it is realized by programming in Python language. For the segmentation of various images, the time-consuming performance of the proposed method is also more eye-catching. It took no more than 1 second to segment an image with a size of 576×768. Therefore, considering the segmentation effect and real-time performance, the method proposed in this paper has good application and promotion value, and the application scenarios of engineering practice are broad.

REFERENCES

[1] Junjie Xing, and Minping Jia, "A convolutional neural network-based method for workpiece surface defect detection," *Measurement*, vol. 176, pp109185, 2021

[2] Enea Poletti, Francesca Zappelli, Alfredo Ruggeri, and Enrico Grisan, "A review of thresholding strategies applied to human chromosome segmentation," *Computer Methods and Programs in Biomedicine*, Vol. 108, no. 2, pp679-688, 2012

[3] Lina Lina, David Reynaldo, Danny Danny, and Arlends Chris, "White Blood Cells Detection from Unstained Microscopic Images using Modified Watershed Segmentation," IAENG International Journal of Computer Science, vol. 48, no.4, pp1151-1161, 2021

[4] Vijai Singh, "Sunflower leaf diseases detection using image segmentation based on particle swarm optimization," *Artificial Intelligence in Agriculture*, vol. 3, pp62-68, 2019

[5] L. Bragagnolo, R.V. da Silva, and J.M.V. Grzybowski, "Amazon forest cover change mapping based on semantic segmentation by U-Nets," *Ecological Informatics*, vol. 62, pp101279, 2021

[6] P.D. Sathya, R. Kalyani, and V.P. Sakthivel, "Color image segmentation using Kapur, Otsu and Minimum Cross Entropy functions based on Exchange Market Algorithm," *Expert Systems with Applications*, vol. 172, pp114636, 2021

[7] Ahmad Wahyu Rosyadi, and Nanik Suciati, "Image Segmentation Using Transition Region and K-Means Clustering," IAENG International Journal of Computer Science, vol. 47, no.1, pp47-55, 2020

[8] Rotimi-Williams Bello, Ahmad Sufril Azlan Mohamed, Abdullah Zawawi Talib, Daniel A. Olubummo, and O. Charles Enuma, "Enhanced Deep Learning Framework for Cow Image Segmentation," IAENG International Journal of Computer Science, vol. 48, no.4, pp1182-1191, 2021

[9] Limiao Deng, Juan Li, and Zhongzhi Han, "Online defect detection and automatic grading of carrots using computer vision combined with deep learning methods," *LWT*, vol. 149, pp111832, 2021

[10] Zhichao Liu, and Baida Qu, "Machine vision based online detection of PCB defect," *Microprocessors and Microsystems*, vol. 82, pp103807, 2021

[11] Jianjie Wu, Limei Peng, Jiawen Li, Xinyu Zhou, Jingbing Zhong, Cynthia Wang, and Jun Sun, "Rapid safety monitoring and analysis of foundation pit construction using unmanned aerial vehicle images," *Automation in Construction*, vol. 128, pp103706, 2021

[12] N. Otsu, "A Threshold Selection Method from Gray-Level Histograms," *IEEE Transactions on Systems, Man, and Cybernetics*, vol. 9, no. 1, pp62-66, 1979

[13] J. Kittler, J. Illingworth, "Minimum error thresholding," *Pattern Recognition*, vol. 19, no. 1, pp41-47, 1986

[14] J.N. Kapur, P.K. Sahoo, and A.K.C. Wong, "A new method for gray-level picture thresholding using the entropy of the histogram," *Computer Vision, Graphics, and Image Processing*, vol. 29, no. 3, pp273-285, 1985

[15] M. Portes de Albuquerque, I.A. Esquef, A.R. Gesualdi Mello, and M. Portes de Albuquerque, "Image thresholding using Tsallis entropy," *Pattern Recognition Letters*, vol. 25, no. 9, pp1059-1065, 2004

[16] C.H. Li, and C.K. Lee, "Minimum cross entropy thresholding," *Pattern Recognition*, vol. 26, no. 4, pp617-625, 1993

[17] Bo Lei, and Jiulun Fan, "Multilevel minimum cross entropy thresholding: A comparative study," *Applied Soft Computing*, vol. 96, pp106588, 2020

[18] Jiafu Li, Wenyan Tang, Jun Wang, and Xiaolin Zhang, "A multilevel color image thresholding scheme based on minimum cross entropy and alternating direction method of multipliers," *Optik*, vol. 183, pp30-37, 2019

[19] A. Sgarro, "Informational divergence and the dissimilarity of probability distributions," *Calcolo*, vo. 18, no. 3, pp293-302, 1981

[20] Fangyan Nie, "Tsallis cross-entropy based framework for image segmentation with histogram thresholding," *Journal of Electronic Imaging*, vol. 24, no. 1, pp013002, 2015

[21] M. Sezgin, and B. Sankur, "Survey over image thresholding techniques and quantitative performance evaluation," *Journal of Electronic Imaging*, vol. 13, no, 1, pp146-165, 2004

[22] Jing-Hao Xue, and D. Michael Titterington, "Median-based image thresholding," *Image and Vision Computing*, vol. 29, no. 9, pp631-637, 2011

[23] Yangyang Li, Xiaoyu Bai, Licheng Jiao, and Yu Xue, "Partitioned-cooperative quantum-behaved particle swarm optimization based on multilevel thresholding applied to medical image segmentation," *Applied Soft Computing*, vol. 56, pp345-356, 2017

[24] Y. Zimmer, R. Tepper, and S. Akselrod, "A two-dimensional extension of minimum cross entropy thresholding for the segmentation of ultrasound images," *Ultrasound in Medicine & Biology*, vol. 22, no. 9, pp1183-1190, 1996